Carbohydrate Polymers 90 (2012) 1069–1074

Contents lists available at SciVerse ScienceDirect

Carbohydrate Polymers

journal homepage: www.elsevier.com/locate/carbpol

Carboxymethyl chitin/organic rectorite composites based nanofibrous mats and their cell compatibility

Shangjing Xin[a,1], Yuejun Li[b,1], Wei Li[a], Jing Du[a], Rong Huang[a], Yumin Du[c,**], Hongbing Deng[a,c,*]

[a] College of Food Science and Technology and the MOE Key Laboratory of Environment Correlative Dietology, Huazhong Agricultural University, No. 1 Shizishan Road Wuhan 430070, China
[b] Department of Plastic Surgery, Tangdu Hospital, Fourth Military Medical University, Xi'an 710038, China
[c] Department of Environmental Science, College of Resource and Environmental Science, Wuhan University, Wuhan 430079, China

ARTICLE INFO

Article history:
Received 29 March 2012
Received in revised form 3 May 2012
Accepted 14 June 2012
Available online 23 June 2012

Keywords:
Carboxymethyl chitin
Poly (vinyl alcohol)
Organic rectorite
Nanofibrous mats
Cell compatibility

ABSTRACT

In this study, carboxymethyl chitin (CMC) - organic rectorite (OREC)/poly (vinyl alcohol) (PVA) composite nanofibrous mats were successfully prepared via electrospinning. SAXRD pattern showed that the interlayer distance of OREC was increased from 3.68 to 4.08 nm, which verified that polymer chains were intercalated into the interlayer of OREC. Field emission scanning electron microscopy, Fourier transform infrared spectra and energy-dispersive X-ray spectroscopy were used to characterize the morphology and microcosmic structure of nanofibrous mats. Thermal properties of mats were determined by differential scanning calorimetry. To evaluate the cell compatibility of mats, mouse lung fibroblast (L929) was chosen for cell attachment and spreading assay. The results shows that nanofibrous mats contained OREC have better thermal properties. Besides, the addition of OREC has little effect on the cell compatibility of nanofibrous mats.

1. Introduction

Electrospinning has, compared with other techniques like template synthesis and phase separation, proved to be a versatile and effective method of nanofibrous mats fabrication. It has been widely applied for its high productivity (Greiner & Wendorff, 2007). Electrospinning nanofibers have a 3D structure with pores in micro and sub-micro size, and so far they have been extensively applied in various areas like tissue engineering scaffolds (Deng et al., 2010), wound dressing (Chen, Chang, & Chen, 2008), biochemical sensors (Ding, Wang, Wang, Yu, & Sun, 2010), bacterial inhibition (Deng et al., 2011b) and cosmetic skin masks (Huang, Zhang, Kotaki, & Ramakrishna, 2003). At present, polymer/layered silicate nanofibers together with their potential applications within aerospace, biodegradable materials, catalysis and some other areas alike has been studied because these composite nanofibers can maintain the advantages of nanofibers and are simultaneously of integrated properties of both inorganic and organic materials (Daniel, Deepak, & Emmanuel, 2002, Goettler, Lee, & Thakkar, 2007, Hartmut, 2003). To the best of our knowledge, the biocompatibility of polymers is the first consideration when applied in biomedical area. Therefore, nature polymers like chitin can be an ideal component for the fabrication of nanofibrous mats.

Chitin, which is normally extracted from shellfishes, is the second most abundant polysaccharide in natural environment. It is biodegradable and biocompatible and therefore can be utilized for drug delivery (Mi et al., 2003) and tissue engineering (Freier, Montenegro, Shan Koh, & Shoichet, 2005). However, its poor water solubility (Noh et al., 2006) has restrained the further utilization of chitin nanofibers for biomaterials. Existing studies show that 1,1,1,3,3,3-hexafluoro-2-propanol (HFIP) is normally selected as the solvent of chitin, but unfortunately HFIP is toxic and harmful to the health of environment and humans (Noh et al., 2006). Therefore, the derivatives of chitin with better water solubility have drawn many attentions (Kittura, Prashantha, Sankarb, & Tharanathan, 2002). Carboxymethyl chitin (CMC) has demonstrated broad prospects in food industries (Agulló, Rodríguez, Ramos, & Albertengo, 2003) and tissue engineering (Jayakumar et al., 2011). But unfortunately, CMC is of poor spinnability and it has to be mixed with other polymers during the electrospinning process (Shalumon et al., 2009). Poly (vinyl alcohol) (PVA) is an ideal candidate because of excellent biocompatibility and spinnability. In addition, PVA nanofibers have high tensile and strength,

* Corresponding author at: College of Food Science and Technology, Huazhong Agricultural University, No. 1 Shizishan Road, 430070 Wuhan, China. Tel.: +86 27 87282111; fax: +86 27 87282111.
** Corresponding author. Tel.: +86 27 68778501; fax: +86 27 68778501.
E-mail addresses: duyumin@whu.edu.cn (Y. Du), alphabeita3000@yahoo.com.cn (H. Deng).
[1] Co-first author with the same contribution to this work.

0144-8617/$ – see front matter © 2012 Elsevier Ltd. All rights reserved.
http://dx.doi.org/10.1016/j.carbpol.2012.06.045

tensile modulus, and abrasion resistance due to its highest crystalline lattice modulus (Lee et al., 2004).

Organic rectorite (OREC), as a kind of layered silicate, is modified from rectotite (REC) and of larger interlayer distance and layer aspect ratio compared with montmorillonite (Wang et al., 2006). It is reported that OREC is applied in antibacterial activity (Deng et al., 2012), drug controlled-release system (Xu et al., 2012) and gene delivery (Wang, Pei, Du, & Li, 2008). Based on our previous report, nanofibrous mats mixed with OREC are verified to improve the bacterial inhibition because of the positive potential and the enlarged interlayer distance (Deng et al., 2011a). Therefore, further study to the physical properties and cell compatibility of polymer-OREC intercalated nanofibrous mats and more attention should be given to their further utilization in biomedical areas.

In this study, CMC/PVA chains were intercalated into the interlayer of OREC to fabricate composite nanofibrous mats by using of electrospinning technique. The study to cell compatibility of polymer-OREC intercalated nanofibrous mats was initiative and no similar studies were reported yet. Means like Fourier transform infrared (FT-IR), energy-dispersive X-ray spectroscopy (EDX) and Field-Emission Scanning Electron Microscope (FE-SEM) were broadly applied for the characterization of prepared fibrous mats. The interlayer distance of OREC was measured by small angle X-Ray diffraction. Differential scanning calorimetry (DSC) was applied to investigate the thermal properties of the composite nanofibrous mats.

2. Materials and methods

2.1. Materials

Chitin ($M_w = 1.31 \times 10^6$ kD) was provided by Yuhuan Ocean Biochemical Co. (Taizhou, China). Poly (vinly alcohol) ($M_w = 9 \times 10^4$ kD) was purchased from Wako Pure Chemical Industries, Japan. Calcium rectorite (Ca^{2+}-REC) was provided by Hubei Mingliu Inc. Co. (Wuhan, China). Organic rectorite was prepared based on a previous report (Wang, Du, Luo, Lin, & Kennedy, 2007). All other chemicals were of analytical grade and used as received. All aqueous solutions were prepared by using purified water with a resistance of 18.2 MΩ cm.

2.2. Preparation of carboxymethyl chitin

Chitin (100 g) was frozen for 12 h at −18 °C after alkalified by 50% NaOH (200 g). Then the solution was thawed by adding 1000 ml Isopropyl Alcohol (IPA) and stirred at room temperature. Chloroacetic acid (110 g) was dissolved into 500 ml IPA and instilled into the prepared solution. This reaction was kept for triple 2 h at 20 °C, 60 °C, 40 °C, respectively. After that, the pH value was adjusted to neutral. The solution was washed by methyl alcohol and dialyzed in 2000 ml distilled water for a week. After rotating evaporation and lyophilization, CMC powder was obtained.

2.3. Preparation of electrospinning solutions and nanofibers

CMC (7%) and PVA (8%) solutions were mixed in different mass ratios of CMC/PVA at 60/40, 50/50, 40/60 and 20/80. CMC-OREC solutions were prepared by dissolving CMC-OREC composites and stirring for 2 h at room temperature. Then PVA solutions were mixed to make sure that the concentration of OREC was 1%.

Custom-designed electrospinning equipment was consisted of a high voltage DC power supply (DW-P303-1ACD8, Tianjing Dongwen high voltage power supply Co., Tianjing, China) and a syringe pump (LSP02-1B, Baoding Longer Precision Pump Co., Ltd., China). The prepared solution was poured into a 10 ml syringe with a metal needle (the inner diameter was 0.8 mm) and driven by the syringe pump. All electrospinning experiments were carried out under a consistent electric field of 10 kV/8 cm. The ambient temperature and relative humidity were maintained at 25 °C and 45%, respectively. The prepared fibrous mats were dried in vacuum at room temperature.

2.4. Characterization

The morphology of electrospun fibrous mats was observed by Field Emission Scanning Electron Microscope (FE-SEM, S-4800, Hitachi Ltd., Japan). All the samples were processed by vacuum spray carbon prior to FE-SEM imaging. The composition of fibrous mats was investigated by energy-dispersive X-ray (EDX) spectroscopy (S-4800, Hitachi Ltd., Japan). Fourier transform infrared (FT-IR) spectra were recorded by a Nicolet FT-IR 5700 spectrophotometer (Nicolet, Madison, USA). The number of FT-IR scans was 64 times. The small angle X-ray diffraction (SAXRD) was performed using D8 Advance diffractometer (Bruker, USA). The scanning rate and the scanning scope of 2θ were 1°/min and 1–10°, respectively. The thermal properties of composite nanofibrous mats were determined by differential scanning calorimetry (DSC 204 F1, Netzsch, Germany) from 20 to 400 °C with a heating rate of 10 °C/min under nitrogen flow 20 ml/min. This experiment was heated up twice to remove the thermal history of samples.

2.5. MTT assay

The cytotoxicity of nanofibrous mats was determined by MTT assay corresponding to a previous report (Zhao et al., 2009). In short, nanofibrous mats cultivated with L929 cells were washed slightly by phosphate buffered saline (PBS). Then 25 μl MTT was added into each plate at 37 °C for 4 h. After that, DMSO (150 μl) was added to dissolve the MTT formazan purple crystals in 10 min. At last, the absorbance of the solution was measured at 490 nm by using an enzyme linked immunosorbent assay (ELISA) Reader (MODEL550, Bio-Rad, USA).

2.6. Cell attachment and spreading assay

Mouse lung fibroblast (L929, provided by Tangdu Hospital, Fouth Military Medical University) was selected to investigate the cell compatibility of composite nanofibrous mats. The mats were cut into small disks to fit the size of 96-well plates and then sterilized by high pressure at 121 °C. L929 cells (1×10^3) in Dulbecco modified eagle medium (DMEM) were seeded onto the nanofibrous specimens in the 96-well plate. DMEM was supplemented with 10% fetal bovine serum (FBS) and 1% penicillin/streptomycin. L929 cells grew at 37 °C in an incubator with a humidified atmosphere containing 5% CO_2 for 24 h. FE-SEM images (FE-SEM, JSM-6700F, JEOL, Japan) were taken to observe the morphology of cell attachment and spreading situation.

3. Results and discussion

3.1. FT-IR spectra analysis

Fig. 1 shows the FT-IR spectra of chitin (a) and CMC (b). The peak at 1652 cm^{-1} represented the absorption value of amide I, and the two peaks at 1558 cm^{-1} and 1600 cm^{-1} represented the absorption values of amide II and amino, respectively, which indicated that the degree of deacetylation of chitin was quite low. But in the spectrum of CMC, all these characteristic peaks became broader. The asymmetric stretching vibration of —CH_2— at 2937 cm^{-1}, the stretching vibration of C—O at 1061 cm^{-1}, the absorption peak of C—O—C around 1175 cm^{-1} were all obviously enlarged, indicating the high degree of substitution of CMC. There was no remarkable

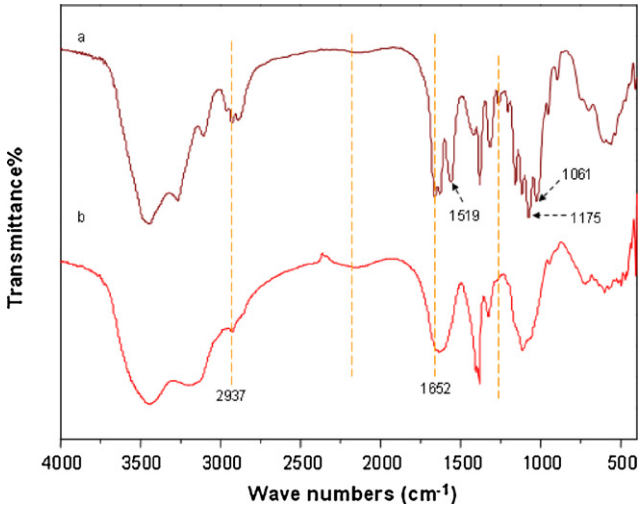

Fig. 1. FT-IR spectra of (a) chitin and (b) CMC.

peak at 1519 cm^{-1} of the free amino which verified that CMC was successfully synthesized.

Fig. 2 presents the FT-IR spectra of CMC-OREC/PVA composite fibrous mats and their raw materials. The characteristic peaks of OREC were at 467 cm^{-1} and 546 cm^{-1} represented for the bending vibration absorption peak of Si—O (Deng et al., 2011b). And the characteristic peaks at 910 cm^{-1} and 3643 cm^{-1} stood for the vibration absorption peak of —OH. The peaks of $-CH_2-$ and $-CH_3$ groups at 2921 cm^{-1} and 2851 cm^{-1} were resulted from sodium dodecylsulphate (SDS) modification of OREC. In the spectrum of PVA, the characteristic peaks of 3383 cm^{-1}, 2941 cm^{-1}, 1734 cm^{-1}, 1098 cm^{-1} and 850 cm^{-1} represented —OH, $-CH_3$, C=O, C—O and C—C, respectively.

The peaks of Si—O at 467 cm^{-1} and 546 cm^{-1} could be seen in the spectra of PVA/OREC (Fig. 2a) and CMC-OREC/PVA mats (Fig. 2c). Besides, the peak of —OH narrowed down at 910 cm^{-1} and even disappeared at 3643 cm^{-1}, which indicated that the hydroxyl group of OREC had interaction with CMC and PVA.

3.2. Morphology of fibrous mats

The morphology of CMC/PVA fibrous mats in different mass ratios is displayed in Fig. 3. The solutions could not be electrospun into fibers when the mass ratio of CMC/PVA was higher than 60/40 according to a previous report (Shalumon et al., 2009). When the mass ratio of CMC/PVA was 60/40 (Fig. 3a), there were many spindle-like beads among the nanofibrous mats and the fibers were primarily embedded in adhesive films because of the bad electrospinability of CMC. When the concentration of PVA increased, the morphology of nanofibrous mats became better. Moreover, the average diameter of nanofibers increased after the addition of PVA. The reason was that PVA was easily to be electrospun and its nanofibers were denser and of larger average diameter. Some adjacent fibers became adhesive because the solvent was distilled water which was hard to be evaporated during such a short electrospinning period.

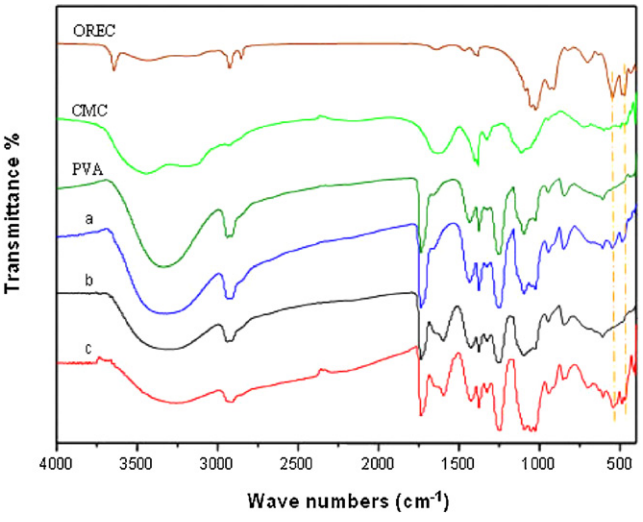

Fig. 2. FT-IR spectra of nanofibrous mats electrospun from different solution component: (a) PVA/OREC, (b) PVA/CMC and (c) CMC-OREC/PVA.

Fig. 4 gives the FE-SEM images of OREC contained composite nanofibrous mats. Their variation of morphology was identical with that of CMC/PVA nanofibrous mats when the mass ratio of CMC/PVA was changed. Compared to Fig. 3a, however, there was no remarkable adhesion among fibers in Fig. 4a because of the existence of OREC. With the addition of OREC, the dissolving rate of nanofibers on the receptor became lower and the solvent evaporated more quickly, because both the internal and external surface of OREC were changed from hydrophilic to hydrophobic after the organification of rectorite (Wang et al., 2007). Furthermore, the nanofibers had better morphology and narrowly distributed diameter (Ray & Okamoto, 2003). The above results elucidates that OREC can affect the morphology of the nanofibrous mats.

3.3. Composition analysis of nanofibrous mats

It is already known that the characteristic elements of OREC are consist of Si and Al. EDX spectrum is used for verifying the existence of OREC in the CMC-OREC/PVA composite nanofibrous mats. The characteristic peaks of Si and Al in the EDX spectrum (Fig. 5) proved that OREC had been successfully added into the composite nanofibrous mats. The characteristic peak of Na indicated that SDS was in the composite nanofibrous mats which also verified that OREC was successfully fabricated into the composite nanofibrous mats.

3.4. X-ray diffraction investigation

SAXRD patterns of CMC-OREC/PVA composite nanofibrous mats are shown in Fig. 6 and the interlayer distance of OREC is calculated by Bragg's equation. There was no remarkable peak observed in CMC, PVA and CMC/PVA composite nanofibrous mats (Fig. 6a–c). The intensity zenith of OREC (Fig. 6d) was at 2.40° and the interlayer distance was 3.68 nm. Compared to OREC, the peaks of PVA-OREC composite nanofibrous mats and CMC-OREC/PVA nanofibrous mats (Figs. 6e and f) shifted towards lower angles at 2.10° and 2.16°, and the interlayer distance were 4.20 and 4.08 nm, respectively. This result indicates that PVA chains are successfully intercalated into the interlayer of OREC but CMC chains have no remarkable effect on intercalation.

3.5. Different scanning calorimetry assay

The thermal properties of nanofibrous mats are demonstrated in Fig. 7. The endothermic peak at 263.2 °C represented the melting peak of CMC (Kittura et al., 2002). This peak of CMC did not shift after adding OREC but the peak area representing enthalpy change was obviously enlarged which indicated that OREC had remarkable effect on the thermal stability of CMC crystallization. This result was identical with the X-Ray diffraction assay that CMC chains were not intercalated into the interlayer of OREC and the

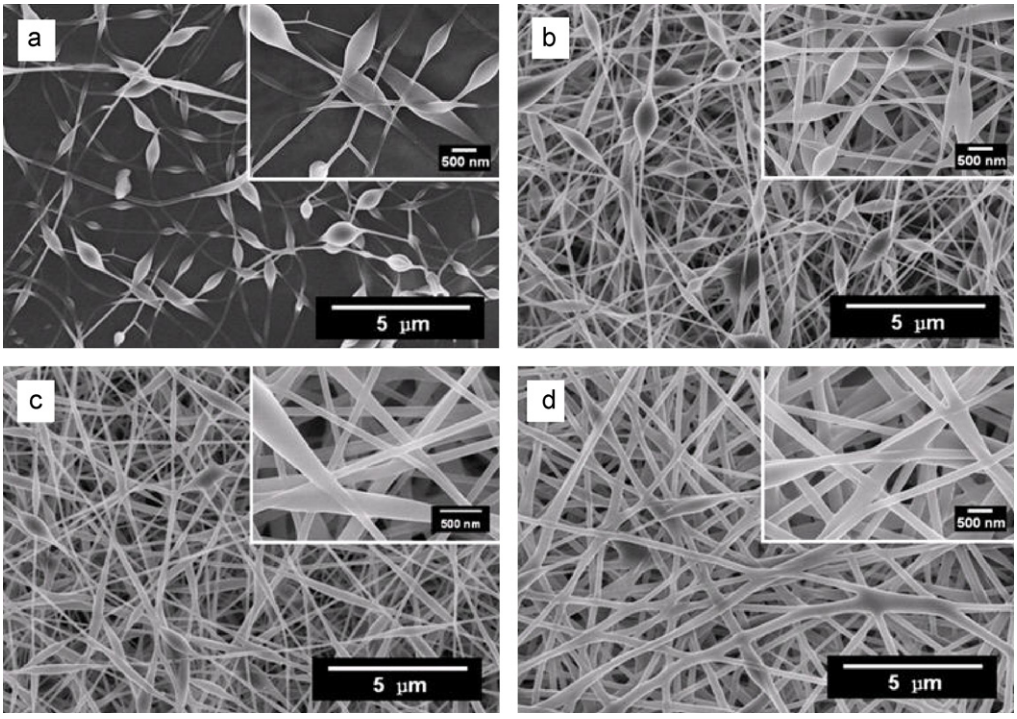

Fig. 3. FE-SEM of nanofibrous membranes electrospun from solutions with different CMC/PVA mass ratios: (a) 60/40, (b) 50/50, (c) 40/60 and (d) 20/80.

crystallization structure of CMC was not destroyed. Besides, the melting peak of PVA at 365 °C in Fig. 7a was more distinct than that of CMC-OREC/PVA nanofibrous mats. In Fig. 7b, the two endothermic peaks did not totally separated, which demonstrated that the crystallization of PVA was destroyed after intercalation. The reason may be that the molecular movements of PVA chains are restricted in a great extent because of the intercalation structure (Wang et al., 2008). As a result, OREC can improve the thermal properties of the nanofibrous mats while not damage the crystallization structure of CMC.

3.6. MTT assay

MTT assay results are shown in Fig. 8a. Obviously, all samples are of slight cytotoxicity. However, the cytotoxicity of the mats contained OREC increased a small amount when the mass ratio of

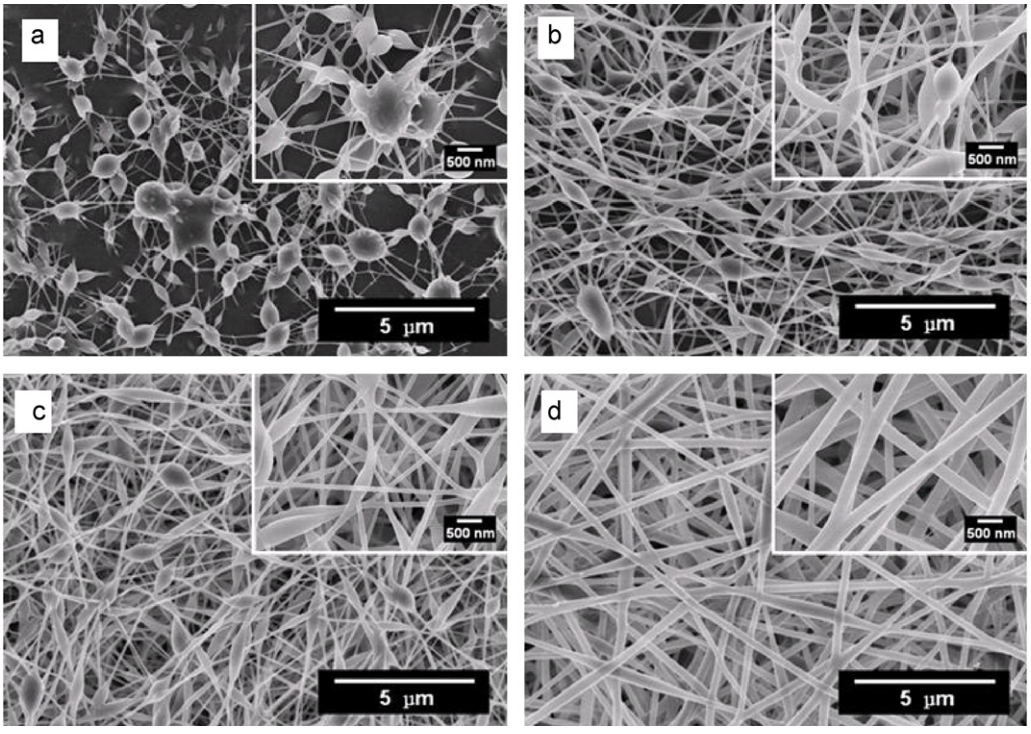

Fig. 4. FE-SEM of nanofibrous membranes electrospun from solutions with different CMC/PVA mass ratios mixed with 1% OREC: (a) 60/40, (b) 50/50, (c) 40/60 and (d) 20/80.

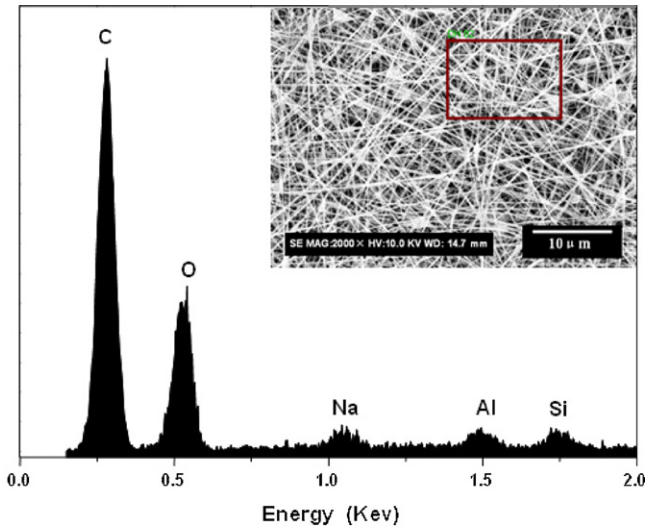

Fig. 5. EDX spectrum of the selected rectangle area of CMC-OREC/PVA nanofibrous mats.

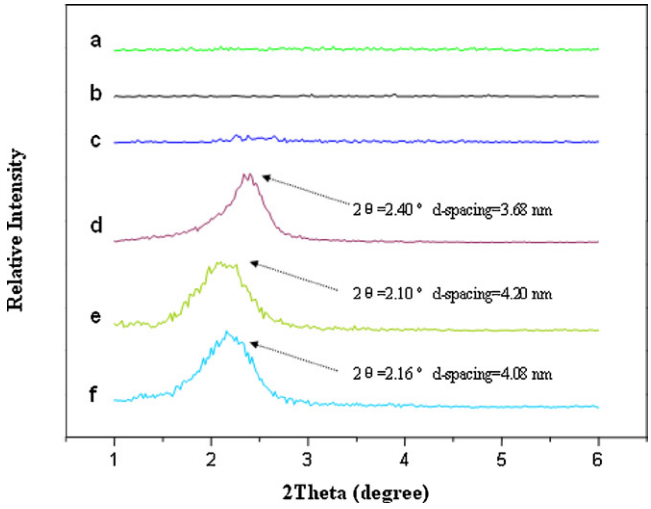

Fig. 6. XRD patterns of samples: (a) CMC powder, (b) PVA nanofibrous mats, (c) CMC/PVA hybrid nanofibrous mats, (d) OREC powder, (e) PVA/OREC nanofibrous mats and (f) CMC-OREC/PVA nanofibrous mats.

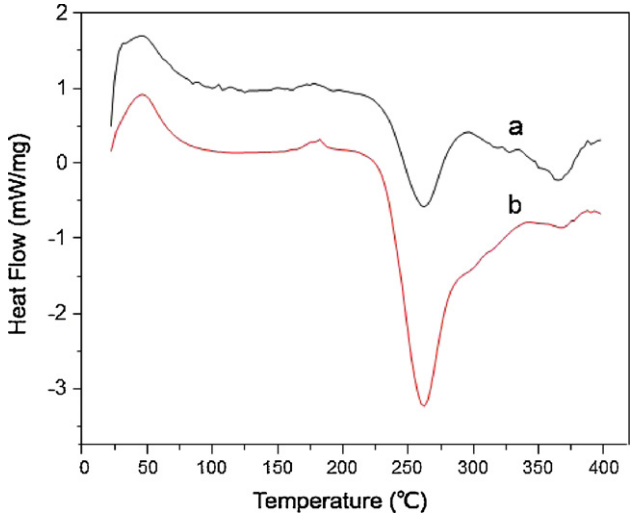

Fig. 7. DSC thermograms of (a) CMC/PVA and (b) CMC-OREC/PVA nanofibrous mats.

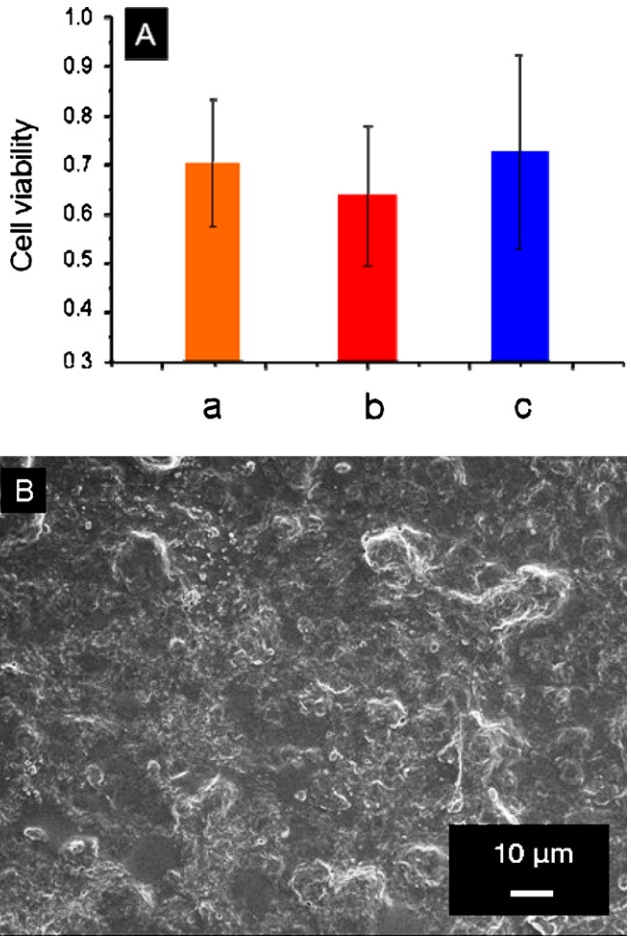

Fig. 8. (A) Cell viability of nanofibrous mats: (a) CMC/PVA = 20/80, (b) CMC/PVA = 20/80 and 1% OREC and (c) CMC/PVA = 40/60 and 1% OREC; (B) FE-SEM images of L929 cell attachment on CMC-OREC/PVA nanofibrous mats (CMC/PVA = 40/60) for 24 h.

CMC/PVA was constant. Besides, when the mass ratio of CMC/PVA read 40/60, the cytotoxicity of nanofibrous mats that contained 1% OREC was less than CMC/PVA (read 20/80) nanofibrous mats, at the same time the thermal properties could be improved with the addition of OREC (Fig. 7). This result may be, according to the DSC results, attributed to the limitation of PVA chains. CMC plays the main role on the cell compatibility after intercalation. Therefore, OREC itself may have a small quantity of cytotoxicity but it helps to reduce that by limiting the movement of PVA chains.

3.7. Cell attachment and spreading assay

The FE-SEM images of L929 cells incubated onto nanofibrous mats for 24 h are demonstrated in Fig. 8b. Because of the outstanding water solubility of CMC and PVA, the fibrous structure of as-spun mats was destroyed after soaking into the cell supernatant, but the destroy was not complete. L929 cells could attach and proliferate well on CMC-OREC/PVA nanofibrous mats, and there were approximate 30 cells in the field of vision. Most cells were with flat morphology and had a size of about 10 μm which verified that they began to split and attached well on the surface of mats. This result shows that CMC-OREC/PVA nanofibrous mats have good cell compatibility and cells can grow well on the mats.

4. Conclusion

In this study, CMC and PVA chains are successfully intercalated into the interlayer of OREC and the composites are electrospun into composite nanofibrous mats. The interlayer distance of OREC increased from 3.68 to 4.08 nm. The thermal properties of nanofibrous mats obviously enhanced and the crystallization of PVA is destroyed after intercalation. MTT assay shows that nanofibrous mats contain OREC has slight toxicity. Mouse lung fibroblasts attach and spread well on the surface of CMC-OREC/PVA nanofibrous mats after 24 h incubation. The developed approach to immobilize layered silicate into polymer nanofibers with controllable interlayer distance can also be used to tailor the sizes, compositions, and surface properties of other 3D structured materials. Those materials are of enormous utilities in the area of catalysis, sensors, tissue engineering, food packaging and antimicrobial wound dressing.

Acknowledgement

This project was funded by National Natural Science Foundation of China (No. 31101365) and the Major State Basic Research Development Program of China (973 Program) (No. 2010CB732204). Partially supported by the Fundamental Research Funds for the Central Universities of China (No. 52902-0900202208).

References

Agulló, E., Rodríguez, M. S., Ramos, V., & Albertengo, L. (2003). Present and future role of chitin and chitosan in food. *Macromolecular Bioscience*, *3*, 521–530.

Chen, J., Chang, G., & Chen, J. (2008). Electrospun collagen/chitosan nanofibrous membrane as wound dressing. *Colloids and Surfaces a-Physicochemical and Engineering Aspects*, *313*, 183–188.

Daniel, S., Deepak, S., & Emmanuel, G. (2002). New advances in polymer/layeredsilicate nanocomposites. *Current Opinion in Solid State and Materials Science*, *6*, 205–212.

Deng, H., Zhou, X., Wang, X., Zhang, C., Ding, B., Zhang, Q., et al. (2010). Layer-by-layer structured polysaccharides film-coated cellulose nanofibrous mats for cell culture. *Carbohydrate Polymers*, *80*, 474–479.

Deng, H., Lin, P., Xin, S., Huang, R., Li, W., Du, Y., et al. (2012). Quaternized chitosan-layered silicate intercalated composites based nanofibrous mats and their antibacterial activity. *Carbohydrate polymers*, *89*, 307–313.

Deng, H., Li, X., Ding, B., Du, Y., Li, G., Yang, J., et al. (2011). Fabrication of polymer/layered silicate intercalated nanofibrous mats and their bacterial inhibition activity. *Carbohydrate Polymers*, *83*, 973–978.

Deng, H., Wang, X., Liu, P., Ding, B., Du, Y., Li, G., et al. (2011). Enhanced bacterial inhibition activity of layer-by-layer structured polysaccharide film-coated cellulose nanofibrous mats via addition of layered silicate. *Carbohydrate Polymers*, *83*, 239–245.

Ding, B., Wang, M., Wang, X., Yu, J., & Sun, G. (2010). Electrospun nanomaterials for ultrasensitive sensors. *Materials Today*, *13*, 16–27.

Freier, T., Montenegro, R., Shan Koh, H., & Shoichet, M. (2005). Chitin-based tubes for tissue engineering in the nervous system. *Biomaterials*, *26*, 4624–4632.

Goettler, L., Lee, K., & Thakkar, H. (2007). Layered silicate reinforced polymer nanocomposites: Development and applications. *Polymer Reviews*, *47*, 291–317.

Greiner, A., & Wendorff, J. (2007). Electrospinning: A fascinating method for the preparation of ultrathin fibers. *Angewandte Chemie International Edition*, *46*, 5670–5703.

Hartmut, F. (2003). Polymer nanocomposites: From fundamental research to specific applications. *Materials Science and Engineering C*, *23*, 763–772.

Huang, Z., Zhang, Y., Kotaki, M., & Ramakrishna, S. (2003). A review on polymer nanofibers by electrospinning and their applications in nanocomposites. *Composites Science and Technology*, *63*, 2223–2253.

Jayakumar, R., Chennazhi, K. P., Srinivasan, S., Nair, S. V., Furuike, T., & Tamura, H. (2011). Chitin scaffolds in tissue engineering. *International Journal of Molecular Sciences*, *12*, 1876–1887.

Kittura, F., Prashantha, K., Sankarb, K., & Tharanathan, R. (2002). Characterization of chitin chitosan and their carboxymethyl derivatives by differential scanning calorimetry. *Carbohydrate Polymers*, *49*, 185–193.

Lee, J., Choi, K., Ghim, H., Kim, S., Chun, D., Kim, H., et al. (2004). Role of molecular weight of atactic poly(vinyl alcohol) (PVA) in the structure and properties of PVA nanofabric prepared by electrospinning. *Journal of Applied Polymer Science*, *93*, 1638–1646.

Mi, F., Shyu, S., Lin, Y., Wu, Y., Peng, C., & Tsai, Y. (2003). Chitin/PLGA blend microspheres as a biodegradable drug delivery system: A new delivery system for protein. *Biomaterials*, *24*, 5023–5036.

Noh, H., Lee, S., Kim, J., Oh, J., Kim, K., Chung, C., et al. (2006). Electrospinning of chitin nanofibers: Degradation behavior and cellular response to normal human keratinocytes and fibroblasts. *Biomaterials*, *27*, 3934–3944.

Ray, S., & Okamoto, M. (2003). Polymer/layered silicate nanocomposites: A review from preparation to processing. *Progress in Polymer Science*, *28*, 1539–1641.

Shalumon, K., Binulal, N., Selvamurugan, N., Nair, S., Menon, D., Furuike, T., et al. (2009). Electrospinning of carboxymethyl chitin/poly(vinyl alcohol) nanofibrous scaffolds for tissue engineering applications. *Carbohydrate Polymers*, *77*, 863–869.

Wang, X., Pei, X., Du, Y., & Li, Y. (2008). Quaternized chitosan/rectorite intercalative materials for a gene delivery system. *Nanotechnology*, *19*, 375102.

Wang, X., Du, Y., Luo, J., Lin, B., & Kennedy, J. (2007). Chitosan/organic rectorite nanocomposite films: Structure characteristic and drug delivery behaviour. *Carbohydrate Polymers*, *69*, 41–49.

Wang, X., Du, Y., Yang, H., Wang, X., Shi, X., & Hu, Y. (2006). Preparation characterization and antimicrobial activity of chitosan/layered silicate nanocomposites. *Polymer*, *47*, 6738–6744.

Xu, R., Feng, X., Li, W., Xin, S., Wang, X., Deng, H., et al. (2012). Novel polymer-layered silicate intercalated composite beads for drug delivery. *Journal of Biomaterial Science. Polymer Edition*, http://dx.doi.org/10.1163/156856211X619630

Zhao, Q., Ji, Q., Xing, K., Li, X., Liu, C., & Chen, X. (2009). Preparation and characteristics of novel porous hydrogel films based on chitosan and glycerophosphate. *Carbohydrate Polymers*, *76*, 410–416.